Journal Name

ARTICLE

Gd^{3+} Complexes Intercalated into Hydroxy Double Salts as Potential MRI Contrast Agents

Miao Jin,[a] Dominic E.M. Spillane,[b] Carlos F. G. C. Geraldes,[c] Gareth R. Williams,*[a] and S.W. Annie Bligh*[d]

The ion exchange intercalation of two Gd-based magnetic resonance imaging contrast agents into hydroxy double salts (HDSs) is reported. The presence of Gd^{3+} diethylenetriaminepentaacetate and Gd^{3+} diethylenetriaminepenta(methylenephosphonate) complexes in the HDS lattice after intercalation was confirmed by microwave plasma-atomic emission spectroscopy. The structural aspects of the HDS-Gd composites were studied by X-ray diffraction, with the intercalates having an interlayer spacing of 14.5-18.6 Å. Infrared spectroscopy confirmed the presence of characteristic vibration peaks associated with the Gd^{3+} complexes in the intercalation compounds. The proton relaxivities of the Gd^{3+} complex-loaded composites were 2 to 5-fold higher in longitudinal relaxivity, and up to 10-fold higher in transverse relaxivity, compared to solutions of the pure complexes. These data demonstrate that the new composites reported here are potentially potent MRI contrast agents.

Introduction

Magnetic resonance imaging (MRI) plays a prominent role for the investigation of soft tissue abnormalities because of its excellent spatial resolution, noninvasive nature, and use of benign non-ionizing radiation.[1,2] Many Ln[3+] complexes - such as Dy[3+] systems - have slow water proton T_1 relaxation and are unsuitable for use in MRI applications,[3] but Gd^{3+}-based agents are widely regarded as being the most effective contrast agents for MRI.[4,5] In recent years, much effort has been undertaken to integrate Gd^{3+} complexes into nanoparticles including dendrimers,[6,7] carbon nanotubes,[8,9] liposomes,[10,11] micelles[12,13] and inorganic nanoparticles.[14-16] For example, $GdCl_3 \cdot 6H_2O$ has been incorporated into the supercage of zeolite NaY nanoparticles[16] and into hollow silica nanospheres.[17] The relaxivities of these two systems were found to be 3-5 times higher for longitudinal (r_1) and 5-10 times greater for transverse relaxivity (r_2) than the clinically used Magnevist contrast agent ($A_2[Gd(DTPA)(H_2O)]$, where DTPA = diethylenetriaminepentaacetate and A = protonated N-methylglucamine; see Fig. 1(a)). However, unchelated Gd^{3+}

metal ions can potentially escape from the inorganic nanoparticles, leading to toxicity.

Both $[Gd(DTPA)(H_2O)]^{2-}$ and $[Gd(DTPMPH_5)(H_2O)]^{2-}$ (gadolinium diethylenetriaminepenta(methylenephosphonate); Fig. 1b) exist as stable anions, and thus are suitable for incorporation into ion exchange matrices such as layered metal hydroxides.[18,19]
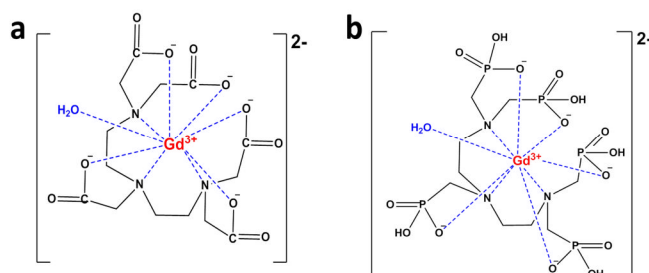

Fig. 1: Schematic structures of (a) $[Gd(DTPA)(H_2O)]^{2-}$ and (b) $[Gd(DTPMPH_5)(H_2O)]^{2-}$.

Layered double hydroxides (LDHs) and hydroxy double salts (HDSs; see **Error! Reference source not found.**) are both layered metal hydroxides (LMH) and can be described with the general formula $[(M^{n+}_aM'^{n+}_b)(OH)_2]X^{n-}_c \cdot zH_2O$. LDHs typically contain divalent and trivalent metal ions, while HDSs are based on two different divalent metal ions, M^{2+} and M'^{2+}. LDHs have been explored as host materials for the intercalation of both near infrared and MRI contrast agents.[20-23] Proton relaxivities four times higher than $[Gd(DTPA)(H_2O)]^{2-}$ for r_1 and 12 times greater for r_2 were observed after the intercalation of $[Gd(DTPA)(H_2O)]^{2-}$ into a Mg/Al LDH.[20] On the other hand, the T_1-weighted map of Zn/Al LDH loaded with $[Gd(DTPA)(H_2O)]^{2-}$ is similar to that of Omniscan[TM] (Gadodiamide), suggesting that

a. UCL School of Pharmacy, University College London, 29-39 Brunswick Square, London, WC1N 1AX, UK.
b. School of Human Sciences, London Metropolitan University, 166-220 Holloway Road, London, N7 8DB, UK.
c. Department of Life Sciences and Coimbra Chemistry Centre, Faculty of Science and Technology, University of Coimbra, Coimbra, Portugal
d. Faculty of Science and Technology, University of Westminster , 115 New Cavendish Street, London, W1W 6UW

intercalation does not yield significant enhancement in this case.[24] In other work, a layered metal hydroxide built from Gd^{3+}, $[Gd_2(OH)_5(H_2O)_x]Cl$, has been synthesized and reported to have a lower r_1 value than $[Gd(DTPAH_2)(H_2O)]$.[25]

Similarly to LDHs, HDSs can potentially be used for the storage and delivery of diagnostic agents through ion exchange intercalation. The electrostatic interaction between the intercalated Gd^{3+} complex and the metal ions in the layer might be expected to extend the rotational lifetime and shorten the relaxation times of bound water protons. In this work we explored the use of HDSs based on Zn^{2+} and Ni^{2+} to incorporate the paramagnetic complexes $[Gd(DTPA)(H_2O)]^{2-}$ and $[Gd(DTPMPH_5)(H_2O)]^{2-}$, and investigated the potential of these HDS-Gd complex nanocomposites as MRI contrast agents.

Results and discussion

Incorporation of $[Gd(DTPA)(H_2O)]^{2-}$ / $[Gd(DTPMPH_5)(H_2O)]^{2-}$ into the HDS interlayer

The Gd complexes were successfully intercalated into the $[Ni_2Zn_3(OH)_8](NO_3)_2 \cdot 2H_2O$ (Ni_2Zn_3-NO_3) HDS, producing Ni_2Zn_3-$Gd(DTPA)/Gd(DTPMPH_5)$. This is shown schematically in Fig. 2.
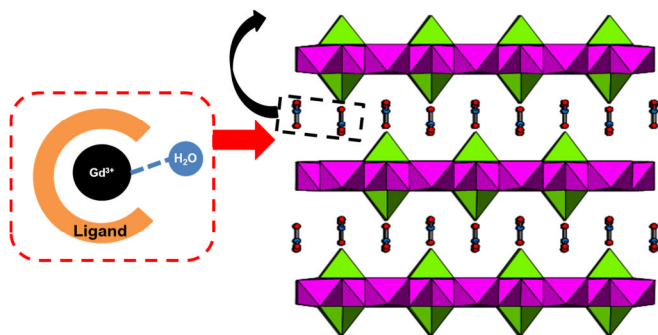

Fig. 2: A schematic illustration of the intercalation of Gd complexes into an HDS. $M(OH)_6$ octahedra are in purple and $M(OH)_4$ tetrahedra in green. Nitrate ions can be seen between the layers.

A systematic variation in the reaction conditions was undertaken, with experiments performed for different amounts of time (1, 3, or 7 day(s)) and with varying molar ratios of HDS: Gd complex. In the interest of brevity we will discuss selected samples in this paper; the experimental conditions used to prepare these are given in Table 1. Details of the full range of materials generated may be found in the Supplementary Information (ESI), Table S1.†

Table 1: Experimental conditions used to prepare selected Gd complex intercalates.

Sample	Complex	Molar ratio [Ni_2Zn_3-NO_3: Gd complex]	Reaction time / day(s)
D1	Gd(DTPA)	5 : 1	7
D5	Gd(DTPA)	5 : 1	3
D9	Gd(DTPA)	5 : 1	1
P1	Gd(DTPMPH_5)	5 : 1	3
P4	Gd(DTPMPH_5)	5 : 1	1

The resultant composites were characterized by powder X-ray diffraction, infrared spectroscopy, and elemental analysis.

In order to evaluate the influence of the paramagnetic Ni(II) ion, a selection of analogous materials were prepared with the all-Zn HDS $[Zn_5(OH)_8](NO_3)_2 \cdot 2H_2O$.

Powder X-ray diffraction

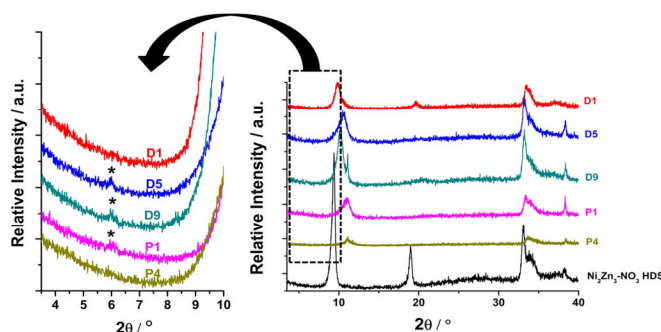Powder X-ray diffraction (XRD) patterns of Ni_2Zn_3-NO_3 and the HDS after reaction with $[Gd(DTPA)(H_2O)]^{2-}$ or $[Gd(DTPMPH_5)(H_2O)]^{2-}$ are presented in Fig. 3.

Fig. 3: X-ray diffraction patterns for the products of selected reactions between Ni_2Zn_3-NO_3 and $[Gd(DTPA)(H_2O)]^{2-}$ ("D" samples) and $[Gd(DTPMPH_5)(H_2O)]^{2-}$ ("P" samples), with intercalate reflections marked with *.

The interlayer spacing of Ni_2Zn_3-NO_3 is 9.7 Å, as reported in the literature.[26] The XRD patterns of Ni_2Zn_3-NO_3 after reaction with $[Gd(DTPA)(H_2O)]^{2-}$ or $[Gd(DTPMPH_5)(H_2O)]^{2-}$ in some cases (D5, D9 and P1) show additional reflections at around 6°, corresponding to interlayer spacings between 14.5 and 14.8 Å. These reflections are attributed to the formation of a Ni_2Zn_3-$Gd(DTPA)$ or Ni_2Zn_3-$Gd(DTPMPH_5)$ phase. The most intense reflection in the HDS/Gd complex patterns can be seen to broaden and shift to higher angle when compared to the starting material: typical interlayer spacings after intercalation are *ca.* 7.7 Å. This is typical of carbonate-containing materials, suggesting that the initial nitrate may have been replaced by carbonate during reaction.[20,27] In D9, two distinct phases can be seen at 8.6 and 7.7 Å. This possibly indicates the presence both of un-exchanged nitrate and carbonate anions.

However, not all the samples (D1 and P4 being examples) present reflections at angles below 10°. This could be because small amounts of $[Gd(DTPA)(H_2O)]^{2-}$ or $[Gd(DTPMPH_5)(H_2O)]^{2-}$ are incorporated into many interlayer spaces, and as a result there is no wholesale expansion of the interlayer spacing, or possibly there are significant amounts of Gd^{3+} complexes adsorbed to the outside of the layers rather than being intercalated.[20,28] Similar finding have been seen in the work of Xu *et al.*, which reported some $[Gd(DTPA)(H_2O)]^{2-}$ to be located on the surface of an Mg/Al LDH post-intercalation.[20] It is clear that a longer reaction time (e.g. D1, 7 days cf. D9, 1 day) does not improve the crystallinity of the solid or result in more intense intercalate reflections.

Infrared spectroscopy

IR spectra of Ni_2Zn_3-NO_3, $Gd(DTPAH_2)(H_2O)$, $Gd(DTPMPH_7)(H_2O)$ and Ni_2Zn_3-NO_3 intercalated with the Gd^{3+} complexes are illustrated in Fig. 4.
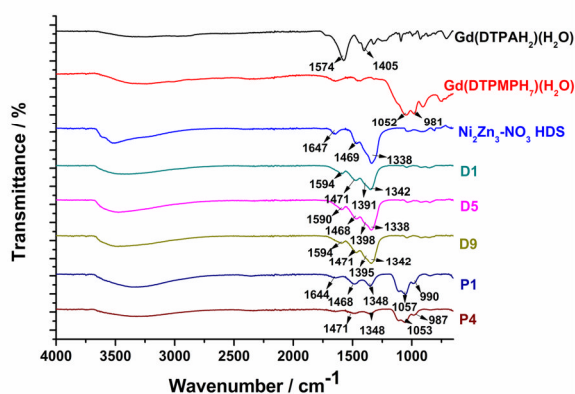
Fig. 4: IR spectra of Gd(DTPAH$_2$)(H$_2$O), Gd(DTPMPH$_7$)(H$_2$O), Ni$_2$Zn$_3$-NO$_3$ and its intercalates with [Gd(DTPA)(H$_2$O)]$^{2-}$ (D1, D5, D9) or [Gd(DTPMPH$_5$)(H$_2$O)]$^{2-}$ (P1, P4).

For the Ni$_2$Zn$_3$-NO$_3$ HDS, the broad band from 3700 to 2700 cm^{-1} is associated with H-bonded O-H stretching vibrations. The peak at 1647 cm^{-1} is attributed to the delta-bend of interlayer water. The vibrational stretching of the free nitrate group is separated into two bands at 1469 cm^{-1} and 1338 cm^{-1} respectively. This indicates NO$_3^-$ is coordinating to metal ions within the layers.[29,30] The absorption peaks below 1000 cm^{-1} are assigned to M-O vibrations and M-O-H bending.[31] The spectrum of Gd(DTPAH$_2$)(H$_2$O) shows characteristic absorption peaks at 1574 cm^{-1} and 1405 cm^{-1} due to the asymmetric and symmetric COOH stretching vibrations.[20] The characteristic peaks at 1052 cm^{-1} and 981 cm^{-1} for Gd(DTPMPH$_7$)(H$_2$O) are associated with v(P=O) and v(P-OH).[32]

Absorption peaks at 1590-1594 cm^{-1} and a broad shoulder on the nitrate peak at around 1400 cm^{-1} emerge after the incorporation of [Gd(DTPA)(H$_2$O)]$^{2-}$ in D1, D5 and D9. For the [Gd(DTPMPH$_5$)(H$_2$O)]$^{2-}$ systems, peaks at 1057/1053 and 990/987 cm^{-1} from the phosphonate groups of the complex can be seen. The strong band at *ca.* 1348 cm^{-1} in the DTPMP intercalates is believed to be a result of carbonate incorporation during the ion exchange process, also suggested by XRD. The peak shifts from 1574 cm^{-1} in Gd(DTPAH$_2$)(H$_2$O) to 1590/1594 cm^{-1} in Ni$_2$Zn$_3$-Gd(DTPA) (D1, D5 and D9), and from 1052 cm^{-1} in Gd(DTPMPH$_7$)(H$_2$O) to 1053/1057 cm^{-1} in Ni$_2$Zn$_3$-Gd(DTPMPH$_5$) (P1 and P4) arise because of electrostatic and hydrogen bonding interactions between the carboxylate / phosphonate groups and the HDS layers.[20] These results confirm the presence of [Gd(DTPA)(H$_2$O)]$^{2-}$ / [Gd(DTPMPH$_5$)(H$_2$O)]$^{2-}$ in the HDS particles.

Elemental analysis

Elemental analysis data for selected Ni$_2$Zn$_3$-Gd(DTPA) and Ni$_2$Zn$_3$-Gd(DTPMPH$_5$) materials are listed in Table 2.

Table 2: Chemical formulae of the Ni$_2$Zn$_3$-NO$_3$ intercalates

Sample	Chemical formula
D1	[Ni$_2$Zn$_3$(OH)$_8$](GdC$_{14}$H$_{18}$O$_{10}$N$_3$)$_{0.09}$·[(NO$_3$)+1/2(CO$_3$)]$_{1.82}$·nH$_2$O
D5	[Ni$_2$Zn$_3$(OH)$_8$](GdC$_{14}$H$_{18}$O$_{10}$N$_3$)$_{0.05}$·[(NO$_3$)+1/2(CO$_3$)]$_{1.90}$·nH$_2$O
D9	[Ni$_2$Zn$_3$(OH)$_8$](GdC$_{14}$H$_{18}$O$_{10}$N$_3$)$_{0.04}$·[(NO$_3$)+1/2(CO$_3$)]$_{1.92}$·nH$_2$O
P1	[Ni$_2$Zn$_3$(OH)$_8$](GdC$_9$H$_{23}$N$_3$O$_{15}$P$_5$)$_{0.34}$·[(NO$_3$)+1/2(CO$_3$)]$_{1.32}$·nH$_2$O
P4	[Ni$_2$Zn$_{2.5}$(OH)$_8$](GdC$_9$H$_{23}$N$_3$O$_{15}$P$_5$)$_{0.36}$·[(NO$_3$)+1/2(CO$_3$)]$_{0.28}$·nH$_2$O

In all cases (see also Table S1, ESI†), the [Ni]/[Zn] molar ratio is close to that reported in the literature (2/3).[26] In general, the Gd content in Ni$_2$Zn$_3$-Gd(DTPA) increases as expected when increasing the reaction times and rising amounts of [Gd(DTPA)(H$_2$O)]$^{2-}$ are used in the reactions. Only a maximum of about 10 % of the initial nitrate ions are replaced by [Gd(DTPA)(H$_2$O)]$^{2-}$. This incomplete exchange may be a result of competition between Gd^{3+} complexes and CO$_3^{2-}$ in solution, with the latter being preferentially intercalated. The particle sizes were measured by dynamic light scattering, and found to be between approximately 430 and 1040 nm.

Zn$_5$-NO$_3$ intercalates

The Zn$_5$-NO$_3$ intercalates are largely analogous to those prepared from Ni$_2$Zn$_3$-NO$_3$. Their XRD patterns are given in Fig. S1, and with low ratios of HDS : Gd^{3+} complex show very similar traits to the Ni$_2$Zn$_3$-NO$_3$ systems: a small reflection at around 18.4 – 18.6 Å corresponding to intercalation of [Gd(DTPA)(H$_2$O)]$^{2-}$ can be seen. This is somewhat higher than that with Ni$_2$Zn$_3$-NO$_3$, but still consistent with complex intercalation. IR data additionally demonstrate intercalation (Fig. S2, ESI†). and MP-AES shows the presence of Gd in the materials. A summary of the data obtained on the Zn$_5$-NO$_3$ derived materials can be found in Table S2 in the ESI†.

^{1}H NMR Studies of [La(DTPA)(H$_2$O)]$^{2-}$ after de-intercalation

To demonstrate the stability of [Gd(DTPA)(H$_2$O)]$^{2-}$ after intercalation and de-intercalation from the HDS, the non-paramagnetic analogue [La(DTPA)(H$_2$O)]$^{2-}$ was intercalated as a model guest, deintercalated by reaction with CO$_3^{2-}$, and ^{1}H NMR measurements were performed on the recovered complex (Fig. S3, ESI†). [La(DTPA)]$^{2-}$ was found to be intact after intercalation and de-intercalation, which is strongly indicative that [Gd(DTPA)]$^{2-}$ will also be unaffected by incorporation in the interlayer of an HDS.

[Gd(DTPA)(H$_2$O)]$^{2-}$ release profile

The [Gd(DTPA)(H$_2$O)]$^{2-}$ release profiles from selected Ni$_2$Zn$_3$-Gd(DTPA) samples were quantified by measuring the Gd content in solution, and are shown in Fig. 5.
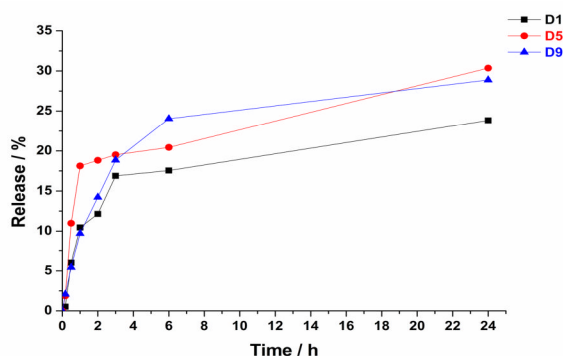
Fig. 5: Release profiles of $[Gd(DTPA)(H_2O)]^{2-}$ from Ni_2Zn_3-Gd(DTPA).

D1 and D9 displayed a relatively rapid release of $[Gd(DTPA)(H_2O)]^{2-}$ (ca. 17 and 18 % respectively) after the first 3 h, followed by more gradual release reaching ca. 23 and 26 % after 24 h. D5 has a similar release pattern, but with a greater burst release of $[Gd(DTPA)(H_2O)]^{2-}$ (ca. 18 % after 1 h), and thereafter a relatively slower release culminating at ca. 30% after 24 h. This burst effect can be explained by the adsorption of some anions on the external structure of the HDS; such ions are rapidly freed into solution.[33] The subsequent slow release step may be largely due to strong electrostatic interactions existing between the HDS layer and the intercalated $[Gd(DTPA)(H_2O)]^{2-}$ anions, which are slowly replaced in an ion-exchange process between the anions in the interlayer and phosphate anions in the buffer.[33,34] $[Gd(DTPA)(H_2O)]^{2-}$, containing five COO^- groups in each ion (and possessing an overall 2- charge), has very strong electrostatic interactions with the HDS layers.[34] It is thus clear that even after extended release times, most of the Gd complexes remain associated with the HDS, and only a minority leaks into solution. Only 4 - 8 % of the Ni and 0.15 - 0.18 % of the Zn contents of the HDSs were released after 24 h (Fig. S4, ESI†), suggesting the layered structure of the HDS remains largely intact under these conditions. Given the infrequency with which MRI diagnostics are generally used on a given patient and the low levels of composite which would be applied, these systems thus do not pose a significant risk of toxicity in terms of excessive Ni or Zn being released into the body (this can cause conditions such as respiratory and cardiovascular systems).[35,36]

Proton relaxivities

The longitudinal (r_1) and transverse (r_2) relaxivities for all the samples are presented in Fig. 6 and 7. Relaxivities were determined from the values of longitudinal ($1/T_1$) and transverse ($1/T_2$) relaxation rates versus the Gd concentration in the HDS suspensions used for measurement.
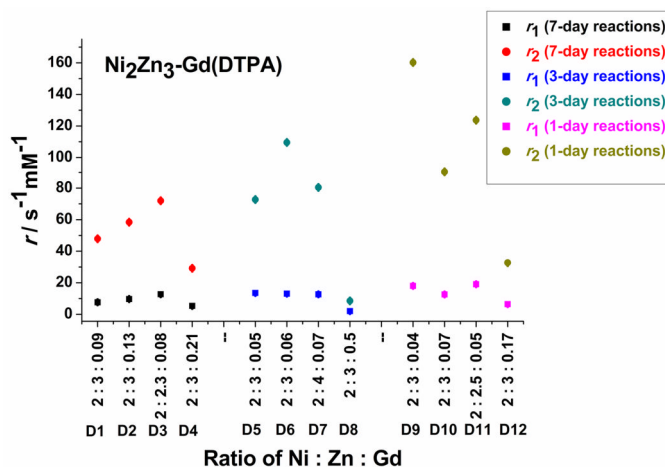

Fig. 6: Relaxivities of Ni_2Zn_3-Gd(DTPA) versus the HDS : complex ratio in the intercalates. Results are reported as mean ± SD, n = 3. Error bars are often so small as to be contained within the symbols.

Fig. 7: Relaxivities of Ni_2Zn_3-Gd(DTPMPH$_5$) versus the HDS : complex ratio of the intercalates. Results are reported as mean ± SD, n = 3. Error bars are often so small as to be contained within the symbols.
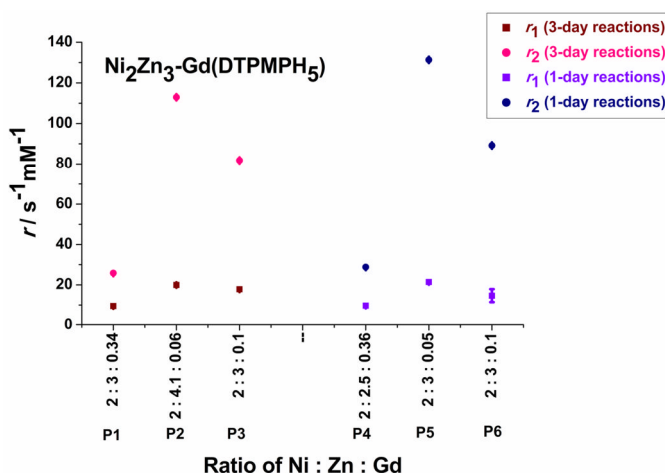
In comparison with the relaxation times of the unloaded all-Zn HDS $[Zn_5(OH)_8](NO_3)_2 \cdot 2H_2O$ (T_1=2806.00 ms, T_2=81.27 ms), the presence of Ni^{2+} in the Ni_2Zn_3-NO_3 HDS is seen to shorten the relaxation times (T_1=532.37 ms, T_2=67.66 ms). Nevertheless, the substitution of paramagnetic ion Ni^{2+} in the HDS did not affect the relaxivities in Ni_2Zn_3-Gd(DTPA) (D5, r_1=13.57 $mM^{-1}s^{-1}$, r_2=72.71 $mM^{-1}s^{-1}$) compared with the data from an analogous Zn_5-Gd(DTPA) system (details given in Table S2, ESI†; for the all-Zn analogue of D1, ZD1: r_1=13.63 $mM^{-1}s^{-1}$, r_2=68.52 $mM^{-1}s^{-1}$) (Table S3, ESI†). This might be due to reduced effectiveness of [Ni-OH] in influencing the relaxation process with the guest complex present.[37,38] While Ni^{2+} can coordinate with water and nitrate ions in the unloaded HDS (therefore affecting relaxivity), it presumably cannot compete with Gd^{3+} for the coordination of water in the intercalates.

For a physical mixture of Ni_2Zn_3-NO_3 and Gd(DTPAH$_2$)(H$_2$O), the r_1 is 9.66 $mM^{-1}s^{-1}$, twice as high as that of Gd(DTPAH$_2$)(H$_2$O), while r_2 = 20.88 $mM^{-1}s^{-1}$ is slightly higher than that of the pure complex. The relaxivity values of all the Gd(DTPA) intercalates (Fig. 6 and 7) are 2-5 times higher for r_1

and up to 10 times greater for r_2 than those of Gd(DTPAH$_2$)(H$_2$O) (r_1=4.5 mM^{-1}s^{-1}, r_2=16.7 mM^{-1}s^{-1}). This is believed to arise as a result of electrostatic interactions between the host matrix and guest ions.

Taking [Gd(DTPA)(H$_2$O)]$^{2-}$ as an example, electrostatic attractions as well as hydrogen bonds between [Gd(DTPA)(H$_2$O)]$^{2-}$ anions and the HDS layers will hold the anions firmly against the positively charged layers. The coordinated oxygen atoms in COO$^-$ groups will be attracted by these interactions away from the nuclear centre (Gd^{3+}) and thus the Gd^{3+}···O coordinated bonds will be weakened. The strengthening of the CO bond in the same COO$^-$ groups could provide compensation for the Gd^{3+}···O bond weakening.[20] This is supported by the shift of the characteristic asymmetric COO$^-$ stretching vibration from 1574 cm^{-1} in Gd(DTPAH$_2$)(H$_2$O) to 1594 cm^{-1} (Fig. 4) in the Ni$_2$Zn$_3$-Gd(DTPA) composites. Meanwhile, the Gd^{3+}···OH$_2$ bond, together with other coordination bonds, is expected to be strengthened.[20] This may cause shortening of the electron-nuclear spin distance, and hence greater communication between the Gd centre and bound water, in turn leading to higher relaxivity.[20] The water exchange rate of the Gd^{3+} complexes is also expected to contribute to relaxivity.[16] The number of water molecules per Gd^{3+} complex in the interlayer is expected to be higher with lower Gd^{3+} complex loadings, leading to more effective exchange and increased relaxivity.[16,20]

With higher Gd loadings, such as in samples D4, D8, D12, P1 and P4 (see Table S1), the observed relaxivity values decrease. This might be because for these intercalates the number of water molecules per Gd^{3+} ion located in the HDS interlayers decreases on increasing the Gd^{3+} loading. Also, the exchange rate of the inner-sphere water molecules with those in the interlayers might become very slow, hence decreasing the relaxation effects. This has similarly been found in Gd-loaded zeolite[16] and liposome systems.[39] In addition carbonate anions, the presence of which was confirmed from XRD and IR data, have a high affinity for Gd^{3+}, leading to possible binding of carbonate to Gd^{3+} centres and the displacement of Gd-bound water.[40] This effect might increase as more Gd complexes are encapsulated into the HDS.

Experimental

Materials

Gadolinium oxide, lanthanum oxide, nickel nitrate, zinc nitrate, and zinc oxide were purchased from Sigma-Aldrich UK. Diethylenetriaminepentaacetic acid was supplied by Alfa Aesar UK. Sodium hydroxide tablets were purchased from Fisher Scientific UK. All other chemicals were of analytical grade and used without further purification. All water used was de-ionised prior to use.

Synthesis

[Ni$_2$Zn$_3$(OH)$_8$](NO$_3$)$_2$·2H$_2$O

The HDS ([Ni$_2$Zn$_3$(OH)$_8$](NO$_3$)$_2$·2H$_2$O) was prepared by the reaction of 9.03 g (0.031 mol) Ni(NO$_3$)$_2$·6H$_2$O and 2.97 g (0.036

mol) of ZnO in 18 cm^3 deionized water. The dispersion was stirred vigorously at room temperature for 7 d. The solid product was recovered by vacuum filtration and washed with water. Finally the solid product was dried in air.

[Zn$_5$(OH)$_8$](NO$_3$)$_2$·2H$_2$O] was prepared using an analogous method to Ni$_2$Zn$_3$-NO$_3$, but using Zn nitrate in place of Ni nitrate.

Gadolinium diethylenetriaminepentaacetate [Gd(DTPAH$_2$)(H$_2$O)]

Gd(DTPAH$_2$)(H$_2$O) was prepared following a literature method.[41] A suspension of 2.83 g (7.2 mmol) diethylene triamine pentaacetic acid and 1.30g (3.6 mmol) gadolinium oxide in 100 cm^3 deionised water was prepared. The mixture was refluxed with stirring for 2 h, after which the solution was clear. The solvent was evaporated by rotary evaporation, after which the solid product was recovered and washed with ethanol and dried under vacuum. (Found: C, 27.00; H, 4.22; N, 6.34%. Calc'd. for GdC$_{14}$H$_{20}$O$_{10}$N$_3$·2.5H$_2$O·0.1Gd$_2$O$_3$: C, 26.74; H, 4.00; N, 6.68%)

Gadolinium diethylenetriaminepenta(methylenephosphonate) [Gd(DTPMPH$_7$)(H$_2$O)]

Gadolinium diethylenetriamine pentamethylenephosphonate was prepared following a literature method.[32] (Found: C, 11.57; H, 3.07; N, 4.24%. Calc'd. for GdC$_9$H$_{25}$N$_3$O$_{15}$P$_5$·1.5H$_2$O·0.5Gd$_2$O$_3$: C, 11.55; H, 3.02; N, 4.49%).

Lanthanum(III)diethylenetriaminepentaacetate[La(DTPAH$_2$)(H$_2$O)]

[La(DTPAH$_2$)(H$_2$O)] was prepared following an analogous method to that used for Gd(DTPAH$_2$)(H$_2$O). (Found: C, 28.59; H, 4.56; N, 6.64%. Calc'd. for LaC$_{14}$H$_{20}$O$_{10}$N$_3$·2.2H$_2$O·1CH$_3$OH·0.088La$_2$O$_3$: C, 28.62; H, 4.55; N, 6.67%)

Intercalation

The [Ni$_2$Zn$_3$(OH)$_8$](NO$_3$)$_2$·2H$_2$O (Ni$_2$Zn$_3$-NO$_3$) host material (0.2 mmol) was suspended in 10 cm^3 of an aqueous solution containing varied amounts of [Gd(DTPA)(H$_2$O)]$^{2-}$ (Table S1, ESI†) and a two-fold molar excess (with respect to [Gd(DTPA)(H$_2$O)]$^{2-}$) of NaOH. The suspension was stirred at 60 °C in an oil bath for a pre-determined period of time (7, 3, or 1 d). The resultant suspension was centrifuged at 2000 rpm for 6 min. The supernatant was discarded, and the solid washed with water, re-suspended, and centrifuged again. This process was repeated three times. Finally, the solid product was dried in an oven at 30 °C for 24 h.

Ni$_2$Zn$_3$-NO$_3$ (0.2 mmol) was loaded with [Gd(DTPMPH$_5$)(H$_2$O)]$^{2-}$ under analogous conditions (Table S1, ESI†). [Zn$_5$(OH)$_8$](NO$_3$)$_2$·2H$_2$O (Zn$_5$-NO$_3$) (0.2 mmol) was similarly loaded with [Gd(DTPA)(H$_2$O)]$^{2-}$ using identical methods to those employed with Ni$_2$Zn$_3$-NO$_3$ (Table S2, ESI†). Ni$_2$Zn$_3$-NO$_3$ / Zn$_5$-NO$_3$ (0.2 mmol) loaded with [La(DTPA)(H$_2$O)]$^{2-}$ (0.1 mmol) were prepared using the same method as for Ni$_2$Zn$_3$-NO$_3$ / [Gd(DTPA)(H$_2$O)]$^{2-}$ (Zn$_5$-NO$_3$ / [Gd(DTPA)(H$_2$O)]$^{2-}$).

X-ray diffraction

X-ray diffraction patterns were recorded over the 2θ range from 3.5 to 40° on a powder diffractometer (PW 1830/40, Philips, Amsterdam, Netherlands) using Cu Kα radiation at 40 kV and 25 mA.

Fourier transform infrared (FTIR) spectroscopy

FTIR analyses were carried out on a Spectrum 100 instrument (PerkinElmer Co. Ltd, Waltham, Massachusetts, USA) over the range 650-4000 cm^{-1} at a resolution of 4 cm^{-1}.

Elemental microanalysis

C, H, and N contents were determined using the combustion method on a Flash 2000 Elemental Analyser (Thermo Scientific, Waltham, Massachusetts, USA).

Microwave plasma-atomic emission spectroscopy

Ni, Zn, and Gd contents were evaluated by microwave plasma-atomic emission spectroscopy (4100 instrument, Agilent Technologies, Santa Clara, California, USA). 10 mg of the sample was placed in a 50 cm^3 of volumetric flask and digested in diluted nitric acid (0.5 %). Linear calibration curves were constructed over the range 1.56-100 ppm and measurements recorded using the following lines: Zn(I) 481.053 nm; Ni(I) 352.454 nm; Gd(II) 342.247 nm, Gd(II) 376.839 nm, Gd(II) 385.097nm, Gd(II) 409.861 nm.

Dynamic light scattering

Measurements were recorded using dynamic light scattering on a Zetasizer Nano ZS instrument (Malvern Instruments, Malvern, UK).

In vitro release test

Approximately 50 mg of D1, D5, or D9 was dispersed in 100 cm^3 of a phosphate buffered saline (PBS; pH 7.4) buffer and stirred at 37 °C. 10 cm^3 aliquots were withdrawn from the buffer at predetermined time points and then replaced by 10 cm^3 of fresh buffer. The samples collected were centrifuged and the metal ion content in the resultant supernatant measured by inductively coupled plasma-optical emission spectroscopy (Optima 4300 DV instrument, Perkin Elmer, Waltham, Massachusetts, USA).

Proton NMR spectroscopy

Approximately 50 mg of the $[La(DTPA)(H_2O)]^{2-}$ intercalates were combined with 100 mg of sodium carbonate and stirred vigorously in 3 cm^3 D_2O overnight. Subsequently the suspensions were centrifuged at 2000 rpm for 6 min. The supernatant was pipetted into NMR tubes. Spectra were recorded on an Avance 400 instrument (^{1}H frequency 400.1 MHz; Bruker, Billerica, Massachusettes, USA).

Proton NMR relaxivity measurements

The longitudinal (T_1) and transverse (T_2) relaxation times of water protons were determined using a Minispec mq20 relaxometer (20 MHz, 0.47 T, Bruker, Billerica, Massachusetts,

USA) at 37 °C, using inversion recovery and CPMG pulse sequences, respectively. 5 mg of the sample was placed in a 10 mm-diameter NMR tube and held using 1 cm^3 1% agarose.

Conclusions

The $[Ni_2Zn_3(OH)_8](NO_3)_2\cdot2H_2O$ hydroxy double salt (HDS) was successfully loaded with Gd^{3+} complexes through ion-exchange intercalation, producing nanocomposites which can be used in MRI. The composites were characterized by X-ray diffraction, IR spectroscopy, microwave plasma-atomic emission spectroscopy (MP-AES) and relaxivity measurements. The partial intercalation of Gd^{3+} complexes into the HDS was evidenced by IR spectra showing characteristic peaks from the complexes, and in some cases X-ray diffraction patterns exhibiting expanded HDS interlayer spacings of *ca.* 14.5 Å. Furthermore, MP-AES results demonstrated the presence of gadolinium in the materials. A selection of analogous materials were prepared with the $[Zn_5(OH)_8](NO_3)_2\cdot2H_2O$ HDS. Certain of the Gd^{3+} complex loaded systems showed much increased longitudinal (r_1; 7.7-21.4 $mM^{-1}s^{-1}$) and transverse (r_2; 25.8-160.2 $mM^{-1}s^{-1}$) proton relaxivities as compared with the free Gd^{3+} complexes. This is not always the case, however, and the highest complex loadings led to the lowest relaxivities (both r_1 and r_2). The Gd^{3+} complexes are believed to remain intact during intercalation and deintercalation on the basis of ^{1}H NMR experiments using the analogous $[La(DTPA)(H_2O)]^{2-}$. Overall, the stability and the enhanced relaxivities of these composites *in vitro* warrant further investigation of their potential as MRI contrast agents *in vivo*.

Acknowledgements

Notes and references

1   P. Caravan, J. J. Ellison, T. J. McMurry, R. B. Lauffer, *Chem. Rev.*, 1999, **99**, 2293-2352.
2   T. Courant, V. G. Roullin, C. Cadiou, M. Callewaert, M. C. Andry, C. Portefaix, C. Hoeffel, M. C. de Goltstein, M. Port, S. Laurent, L. Vander Elst, R. Muller, M. Molinari and F. Chuburu, *Angew. Chem. Int. Ed.*, 2012, **51**, 9119-9122.
3   X. Ma, N. Xu, C. Gao, L. Li, B. Wang, W. Shi and P. Cheng, *Dalton Trans.*, 2015, **44**, 5276-5279.
4   P. Hermann, J. Kotek, V. Kubicek and I. Lukes, *Dalton Trans.*, 2008, 3027-3047.
5   E. Boros, E. M. Gale and P. Caravan, *Dalton Trans.*, 2015, **44**, 4804-4818.
6   Z. L. Cheng, D. L. J. Thorek and A. Tsourkas, *Angew. Chem. Int. Ed.*, 2010, **49**, 346-350.
7   K. Luo, G. Liu, X. W. Zhang, W. C. She, B. He, Y. Nie, L. Li, Y. Wu, Z. R. Zhang, Q. Y. Gong, F. B. Gao, B. Song, H. Ai and Z. W. Gu, *Macromol. Biosci.*, 2009, **9**, 1227-1236.

8   K. B. Hartman, S. Laus, R. D. Bolskar, R. Muthupillai, L. Helm, E. Toth, A. E. Merbach and L. J. Wilson, *Nano Lett.*, 2008, **8**, 415-419.

9   J. H. Choi, F. T. Nguyen, P. W. Barone, D. A. Heller, A. E. Moll, D. Patel, S. A. Boppart and M. S. Strano, *Nano Lett.*, 2007, **7**, 861-867.

10   N. Kamaly, T. Kalber, M. Thanou, J. D. Bell and A. D. Miller, *Bioconjugate Chem.*, 2009, **20**, 648-655.

11   S. Erdogan, A. Roby, R. Sawant, J. Hurley and V. P. Torchilin, *J. Liposome Res.*, 2006, **16**, 45-55.

12   J. Lu, S. L. Ma, J. Y. Sun, C. C. Xia, C. Liu, Z. Y. Wang, X. N. Zhao, F. B. Gao, Q. Y. Gong, B. Song, X. T. Shuai, H. Ai and Z. W. Gu, *Biomater.*, 2009, **30**, 2919-2928.

13   K. Shiraishi, K. Kawano, T. Minowa, Y. Maitani and M. Yokoyama, *J. Controlled Release*, 2009, **136**, 14-20.

14   J. Della Rocca and W. Lin, *Eur. J. Inorg. Chem.*, 2010, 3725-3734.

15   M. F. Ferreira, B. Mousavi, P. M. Ferreira, C. I. O. Martins, L. Helm, J. A. Martins and C. F. G. C. Geraldes, *Dalton Trans.*, 2012, **41**, 5472-5475.

16   C. Platas-Iglesias, L. Vander Elst, W. Z. Zhou, R. N. Muller, C. F. G. C. Geraldes, T. Maschmeyer and J. A. Peters, *Chem. Eur. J.*, 2002, **8**, 5121-5131.

17   W.-I. Lin, C.-Y. Lin, Y.-S. Lin, S.-H. Wu, Y.-R. Huang, Y. Hung, C. Chang and C.-Y. Mou, *J. Mater. Chem. B*, 2013, **1**, 639-645.

18   J.-H. Choy, S.-Y. Kwak, J.-S. Park and Y.-J. Jeong, *J. Mater. Chem.*, 2001, **11**, 1671-1674.

19   A. I. Khan and D. O'Hare, *J. Mater. Chem.*, 2002, **12**, 3191-3198.

20   Z. P. Xu, N. D. Kurniawan, P. F. Bartlett and G. Q. Lu, *Chem. Eur. J.*, 2007, **13**, 2824-2830.

21   Y. Kuthati, R. K. Kankala, C.-H Lee, *Appl. Clay Sci.,* 2015, **112–113**, 100-116.

22   Y.-M. Kuo, Y. Kuthati, R. K. Kankala, P.-R. Wei, C.-F. Weng, C.-L. Liu, P.-J. Sung, C.-Y. Mou and C.-H. Lee, *J. Mater. Chem. B,* 2015, **3**, 3447-3458

23   P.-R. Wei, S.-H. Cheng, W.-N. Liao, K.-C. Kao, C.-F. Weng and C.-H. Lee, *J. Mate. Chem.,* 2012, **22**, 5503-5513.

24   S. Y. Kim, J.-M. Oh, J. S. Lee, T.-J. Kim and J.-H. Choy, *J. Nanosci. Nanotechnol.*, 2008, **8**, 5181-5184.

25   B.-I. Lee, K. S. Lee, J. H. Lee, I. S. Lee and S.-H. Byeon, *Dalton Trans.*, 2009, **14**, 2490-2495.

26   M. Meyn, K. Beneke and G. Lagaly, *Inorg. Chem.*, 1993, **32**, 1209-1215.

27   V. R. L. Constantino and T. J. Pinnavaia, *Inorg. Chem.*, 1995, **34**, 883-892.

28   J.-H. Choy, S.-J. Choi, J.-M. Oh and T. Park, *Appl. Clay Sci.*, 2007, **36**, 122-132.

29   J. P. Auffredic and D. Louer, *J. Solid State Chem.*, 1983, **46**, 245-252.

30   C. Chouillet, J. M. Krafft, C. Louis and H. Lauron-Pernot, *Spectrochim. Acta A Mol. Biomol. Spectrosc.*, 2004, **60**, 505-511.

31   G. G. Carbajal Arizaga, K. G. Satyanarayana and F. Wypych, *Solid State Ionics*, 2007, **178**, 1143-1162.

32   S. W. A. Bligh, C. T. Harding, A. B. McEwen, P. J. Sadler, J. D. Kelly and J. A. Marriott, *Polyhedron*, 1994, **13**, 1937-1943.

33   H. Zhang, K. Zou, S. Guo, X. Duan, *J. Solid State Chem.,* 2006, **179**, 1792-1801.

34   Z. Gu, A. C. Thomas, Z. P. Xu, J. H. Campbell, G. Q. Lu, *Chem. Mater.,* 2008, **20**, 3715-3722.

35   T. Xia, M. Kovochich, M. Liong, L. Mädler, B. Gilbert, H. Shi, J. I. Yeh, J. I. Zink and A. E. Nel, *ACS nano,* 2008, **2**, 2121-2134.

36   E. Denkhaus and K. Salnikow, *Crit Rev Oncol Hematol,* 2002, **42**, 35-56.

37   J. L. Barnhart and R. N. Berk, *Invest. Radio.*, 1986, **21**, 132-136.

38   P. S. Tofts, B. Shuter and J. M. Pope, *Mag. Reson. Imaging*, 1993, **11**, 125-133.

39   J. P. André, E. Toth, H. Fischer, A. Seelig, H. R. Mäcke and A. E. Merbach, *Chem. Eur. J.*, 1999, **5**, 2977-2983.

40   R. A. Caldwell, H. F. Clemo and C. M. Baumgarten, *Am. J. Physiol-Cell Ph*, 1998, **275**, C619-C621.

41   H. J. Weinmann, R. C. Brasch, W. R. Press, G. E. Wesbey, *Am J Roentgenol,* 1984, **142**, 619-624.